A quantum chemical study of H$_2$S$_2$: Intramolecular torsional mode and intermolecular interactions with rare gases

Glauciete S. Maciel,[1,a)] Patricia R. P. Barreto,[2] Federico Palazzetti,[1] Andrea Lombardi,[1] and Vincenzo Aquilanti[1]

[1]*Dipartimento di Chimica, Università di Perugia, 06123 Perugia, Italy*
[2]*Laboratório Associado de Plasma, Instituto Nacional de Pesquisas Espaciais (INPE)/MCT, CEP 12247-97, São José dos Campos, São Paulo, Brazil*

The structural and energetic properties of the H$_2$S$_2$ molecule have been studied using density functional theory, second-order Møller–Plesset method, and coupled cluster theory with several basis sets. In order to extend previous work on intra- and intermolecular dynamics of the chirality changing modes for H$_2$O$_2$ and its derivatives, our focus has been on the torsion around the S–S bond, along with an extensive characterization of the intermolecular potentials of H$_2$S$_2$ with the rare gases (He, Ne, Ar, and Kr). Use is made of previously defined coordinates and expansion formulas for the potentials which allow for a faithful representation of geometrical and symmetry properties of these systems that involve the interaction of an atom with a floppy molecule. The potential energy surfaces obtained in this work are useful for classical and quantum mechanical simulations of molecular collisions responsible for chirality changing processes of possible interest in the modeling of prebiotic phenomena. © *2008 American Institute of Physics.* [DOI: 10.1063/1.2994732]

I. INTRODUCTION

The origin of biological homochirality is one of the most fascinating and elusive questions in modern science. A great deal of work has been devoted to attempts at explaining the prevalence of specific enantiomeric form over the other one, so far with no generally accepted answer. In recent years experimental approaches (see Refs. 1–3) have suggested that factors acting at the macroscopic level, such as in vortices, for example, can induce selectivity in molecular chirality. Based on this information, as well as on ample experimental and theoretical evidence about molecular alignment induced by collision,[4–13] a systematic study has been started on the possible experimental realization of such type of phenomenon.[14–18]

For reasons of simplicity regarding modeling through affordable and yet reliable electronic structure calculations of the interactions and realistic dynamical treatments, our initial focus was on hydrogen peroxide. A series of quantum studies involving H$_2$O$_2$ (Refs. 15, 16, and 18) and its alkyl[16] and halogen derivatives[17] were carried out with the purpose of providing a quantitative picture, which would allow us to describe the intermolecular interactions of these species, particularly with the rare gases, as can be seen in Ref 18. The obtained information serves as a starting point for planning molecular beam experiments. Again within the framework of studies of prototypical molecules as candidates for possible chiral effects induced by collisions in molecular beams, new investigations have been started on a molecule very similar to H$_2$O$_2$, namely H$_2$S$_2$. The choice was dictated from our previous experimental and theoretical work on the interac-

tion of both H$_2$O and H$_2$S with rare gases.[12,19,20] See Refs. 21–24 for previous theoretical studies regarding chirality around the S–S bond for processes involving electron impact or polarized light absorption.

Interest in the structure and dynamics of these compounds is also an aspect of the fact that the spatial orientation of molecules is crucial for biochemical activity; the best known example being perhaps that of the proteins. Specifically, and similarly to the case of the peroxydic bond (–OO–), the disulfide bonds (–SS–) give to molecules where they occur characteristic geometrical configurations, which influence the biochemical—or in general chemical–activity. A reason why nature exploits the (–SS–) bond in order to induce structural rigidity is its high bond energy, the third strongest among the simple homonuclear bonds. In the applications, vulcanization is typical, whereby latex acquires physical properties, which turn out to be adequate for specific mechanical requirements, such as those involved in tires.

However, the SS bond can be viewed as weak when compared with other types of bonds which break or form in chemical reactions. The breaking of the SS bond in RS-SR' types of compounds can take place through the reduction of one electron, thermal dissociation (such as in combustion processes), or through selective excitation of the bond (e.g., photochemical). In the two latter processes, one has the formation of RS radicals. These processes are of great interest in atmospheric science and as such have been amply investigated both experimentally and theoretically, contributing to the elucidation of thermodynamic properties of various disulfides and of the formed radicals.[25]

In Refs. 26 and 27, Quack and co-workers reported quantitative calculations of stereomutation tunneling in H$_2$S$_2$

---

a)Author to whom correspondence should be addressed. Electronic mail: ciete@dyn.unipg.it.

129, 164302-1

TABLE I. Geometries, energies, and dipole moments for the H$_2$S$_2$ with different basis sets and theory levels.

Method	Basis set	R_{H-S} (Å)	R_{S-S} (Å)	$<_{HSS}$ (deg)	$<_{HSSH}$ (deg)	Energy (H)	μ (D)
B3LYP	cc-pVDZ	1.363	2.107	98.1	90.8	−797.618 217 7	1.33
	cc-pVTZ	1.350	2.086	98.4	90.6	−797.656 899 5	1.20
	cc-pVQZ	1.348	2.078	98.6	90.7	−797.666 607 2	1.15
	aug-cc-pVDZ	1.362	2.109	97.9	91.1	−797.626 370 3	1.16
	aug-cc-pVTZ	1.349	2.087	98.4	90.8	−797.658 543 4	1.12
	aug-cc-pVQZ	1.348	2.078	98.6	90.8	−797.667 129 8	1.10
B3PW91	cc-pVDZ	1.361	2.087	98.1	90.8	−797.518 207 4	1.41
	cc-pVTZ	1.350	2.066	98.4	90.7	−797.555 430 0	1.24
	cc-pVQZ	1.348	2.059	98.6	90.7	−797.564 836 9	1.18
	aug-cc-pVDZ	1.361	2.089	97.9	91.1	−797.525 226 0	1.20
	aug-cc-pVTZ	1.350	2.067	98.4	90.9	−797.556 819 5	1.15
	aug-cc-pVQZ	1.348	2.059	98.6	90.8	−797.565 278 5	1.14
MP2(FU)	cc-pVDZ	1.350	2.091	97.7	90.5	−796.505 814 3	1.46
	cc-pVTZ	1.336	2.060	97.8	90.6	−796.689 344 9	1.31
	cc-pVQZ	1.336	2.049	98.0	90.8	−796.777 357 3	1.27
	aug-cc-pVDZ	1.352	2.102	97.2	91.3	−796.534 472 5	1.29
	aug-cc-pVTZ	1.336	2.059	97.7	91.1	−796.704 787 5	1.25
	aug-cc-pVQZ	1.336	2.049	98.0	90.8	−796.783 244 1	1.24
CCSD(T)	cc-pVDZ	1.357	2.110	97.5	90.5	−796.534 481 3	1.46
	cc-pVTZ	1.344	2.082	97.7	90.5	−796.671 479 3	1.30
	cc-pVQZ	1.343	2.067	98.0	90.7	−796.711 435 4	1.27
	aug-cc-pVDZ	1.359	2.121	97.2	91.1	−796.563 669 9	1.29
	aug-cc-pVTZ	1.345	2.084	97.7	90.8	−796.681 645 6	1.24
	aug-cc-pVQZ	1.343	2.067	97.9	90.8	−796.715 102 6	1.24
Expt[a]		1.341	2.061	97.4	90.8		1.17±0.02

[a]Reference 29.

and disulfide isotopomers and predicted a very small influence of weak force parity violation on the energy differences of enantiomers.

This paper reports, in the next section, details of the computational methods employed for the study of the structural properties of the H$_2$S$_2$ molecules, leading to the choice of the theory levels and basis sets to be used subsequently for the characterization of the intermolecular interactions with noble gases. Particularly relevant is the comparison of the torsional energy profile with that of H$_2$O$_2$, both regarding geometrical features and barrier heights. This and other results are reported and discussed in Sec. III, while Sec. IV is devoted to conclusions.

II. COMPUTATIONAL METHODS

A. The H$_2$S$_2$ molecule

In this study, all *ab initio* calculations were performed using the GAUSSIAN03 program.[28] The equilibrium geometry structure of H$_2$S$_2$ have been investigated by density functional theory (DFT), the second order Møller–Plesset perturbation theory using all electrons [MP2(FU)] and coupled cluster [CCSD(T)] method with several basis sets. For density functional calculations, hybrid density functionals were used since they manifestly yielded better results. The exchange and correlation functionals taken together are commonly represented as B3LYP and B3PW91, where (B3) are the Becke's three-parameter exchange function and (LYP) and (PW91) are different sets of correlation functionals (the functional due to Lee, Yang, and Parr and the functional due

to Perdew and Wang, respectively). Results are shown in Table I.

As a heavier-atom analog to hydrogen peroxide (H$_2$O$_2$), the H$_2$S$_2$ molecule is especially interesting both for its similarities to (and differences from) that one. In this work, the torsional potential functions of H$_2$S$_2$ (Fig. 1) at the B3LYP/6-311++G (3*df*, 3*pd*), MP2(FU)/aug-cc-pVTZ and CCSD(T)/aug-cc-pVXZ (*X*=D and T) have been examined and compared (in the following, for simplicity, we present explicit and discuss mainly data from Dunning basis sets).
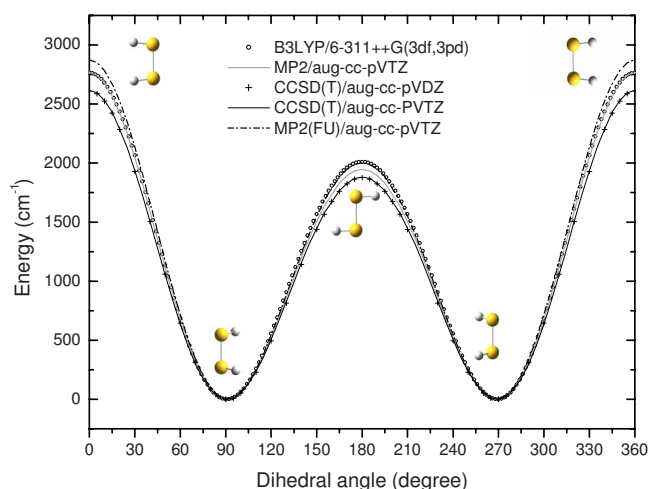

FIG. 1. (Color online) Variation of the energy profile of the H$_2$S$_2$ molecule as a function of dihedral angles for different theory levels and basis sets. The experimental barriers (Ref. 30) are 2800(90) and 1990(15) cm^{-1} for *cis* and *trans* configurations, respectively.
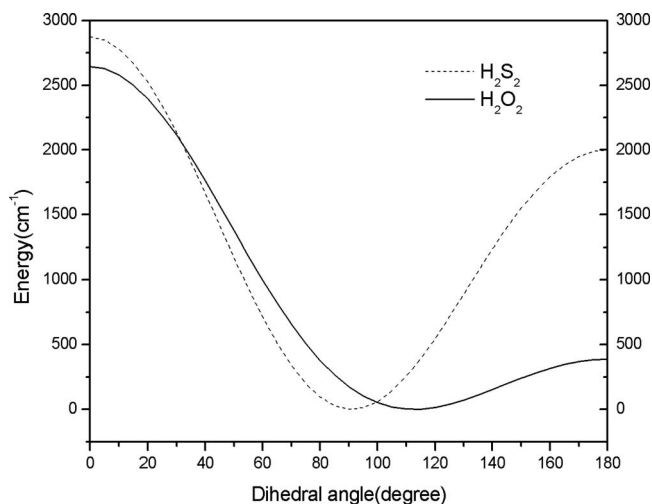
FIG. 2. Variation of the energy of the H$_2$S$_2$ and H$_2$O$_2$ molecules as a function of dihedral angles at MP2(FU)/aug-cc-pVTZ level. The *trans* barrier is higher for H$_2$S$_2$ with respect to that H$_2$O$_2$ (2003.0 vs 386.6 cm^{-1}).

The potentials for both molecules are shown in Fig. 2, using the MP2(FU)/aug-cc-pVTZ method. Figure 3 shows the effect of torsion on dipole moments for both H$_2$O$_2$ and H$_2$S$_2$, while Fig. 4 reports the dependence of dipole moments with the basis sets used. The *cis* and *trans* barriers at several *ab initio* and DFT levels have been determined and presented in Table II.

B. The H$_2$S$_2$-rare gas systems

For the study of H$_2$S$_2$-rare gas systems the second-order Møller–Plesset level, using all electrons [MP2(FU)], and the aug-cc-pVTZ basis set were chosen for He, Ne, Ar, and Kr. To minimize the basis set superposition error, the full counterpoise Boys and Bernardi correction[32] was applied. We calculated a set of 81 single potential energy points on the surface, for each of the eleven leading configurations, to be
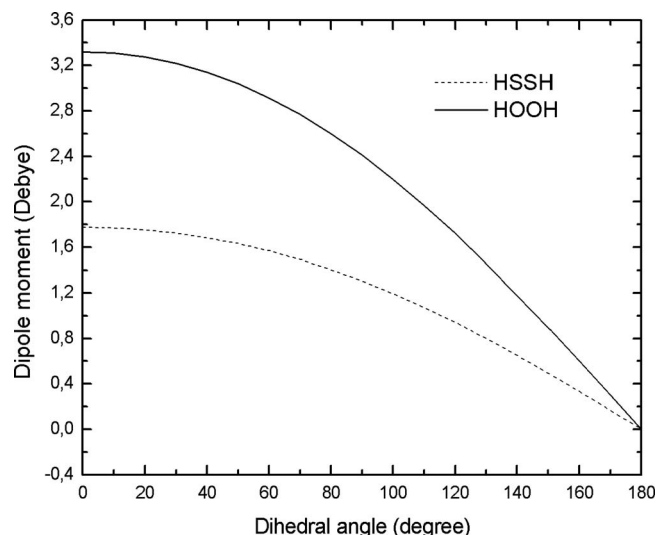

FIG. 3. Variation of dipole moment of the H$_2$S$_2$ and H$_2$O$_2$ molecules as a function of dihedral angles at CCSD(t)/aug-cc-pVDZ level. The experimental values in the equilibrium geometries are 1.17 and 1.57 D for H$_2$S$_2$ and H$_2$O$_2$, respectively.
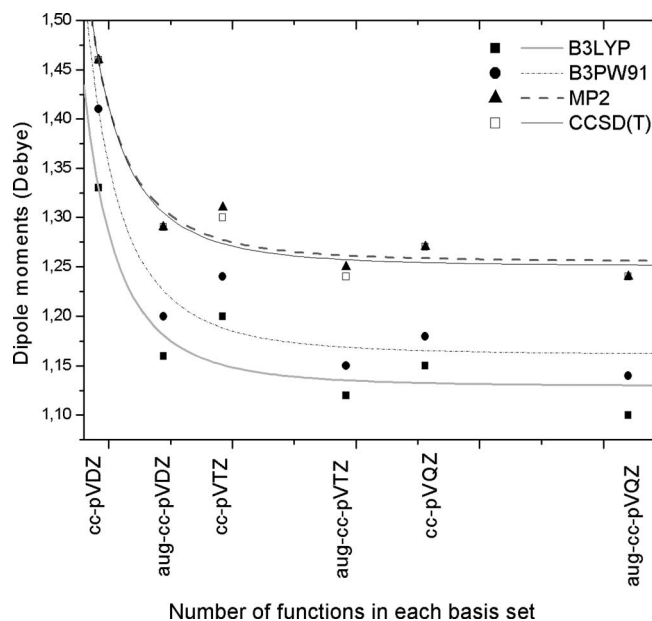

FIG. 4. Effects of basis set on dipole moment for H$_2$S$_2$ at several theory levels. Best fit curves are drawn as an aid for the eye, using formula of the type of Eq. (1) in Ref. 31. The experimental value in the equilibrium geometry is 1.17 D for H$_2$S$_2$.

defined below for H$_2$S$_2$-Rg (Rg=He, Ne, Ar, and Kr). All the H$_2$S$_2$ geometry parameters are kept frozen at their equilibrium values as presented in Tables I and III.

The eleven different leading configurations used to explore the various features of the potential energy surfaces, four for the equilibrium geometry, four for the *cis* geometry, and three for the *trans* geometry, were the same used in H$_2$O$_2$ and have been described in a previous work.[15] For each system, an additional configuration to be introduced later served for assessing the accuracy of the proposed expansion. All energies were calculated as a function of the distance r between the rare gas and the center of mass of H$_2$S$_2$. The analytical forms of the potential energy surfaces, for each of the leading configurations, are constructed by fitting a fifth degree generalized Rydberg function into the *ab initio* points. A nonlinear least-squares procedure was used to obtain the values of the adjustable parameters that minimize the differences between the analytical energies obtained with the generalized Rydberg function and the MP2(FU)/aug-cc-pVTZ data. For additional information, see Ref. 18.

C. Hyperspherical harmonics expansion

Real hyperspherical harmonics and their use to represent the potential energy surface of atom-floppy molecule interactions were widely discussed for the specific case of the H$_2$O$_2$-rare gas system.[18] We use here the same method to represent the interaction of the H$_2$S$_2$-rare gas analogous system.

The reference frame is set in the center of mass of the H$_2$S$_2$ molecule. The position vector r of the rare gas atom is defined by the spherical coordinates (r, α, β), where r is the vector modulus (the distance from the center of mass) and α $(0 \leq \alpha < 2\pi)$ and β $(0 \leq \beta \leq \pi)$ are the azimuthal and

TABLE II. *Cis* and *trans* barriers (cm⁻¹) for the H_2S_2 torsional mode for different basis sets and theory levels.

Methods	B3LYP		B3PW91		MP2(FU)		CCSD(T)	
Basis sets	*Trans*	*Cis*	*Trans*	*Cis*	*Trans*	*Cis*	*Trans*	*Cis*
cc-pVDZ	1802	2631	1900	2781	1833	2733	1762	2576
cc-pVTZ	1925	2669	2022	2806	1985	2831	1895	2642
cc-pVQZ	1961	2703	2062	2842	2026	2870	1958	2714
aug-cc-pVDZ	1843	2558	1966	2734	1950	2767	1877	2610
aug-cc-pVTZ	1889	2624	1998	2770	2003	2873	1886	2622
aug-pVQZ	1942	2686	2046	2827	2034	2879	1957	2706
Expt[a]	*Trans*=1990(15)				*Cis*=2800(90) cm⁻¹			

[a]Reference 30.

polar angle, respectively (Fig. 2). An additional γ variable represents the dihedral angle of the molecule ($0 \leq \gamma < 2\pi$), where $\gamma=0$ corresponds to *cis* geometry and $\gamma=\pi$ to *trans* geometry. Its variation is actually best described as a rotation of the two SH radicals around the Jacobi vector joining their centers of mass,[15] the floppy degree of freedom of the molecule. The *z*-axis is taken along the Jacobi vector and the *xz*-plane that bisects symmetrically the H_2S_2 molecule coincides with the plane of the molecule when $\gamma=0°$ (*cis* geometry) and $\gamma=180°$ (*trans* geometry). The α variable is the angle between the positive *x*-axis and the projection of *r* onto the *xy*-plane, while β is the angle between the positive *z*-axis and the line connecting the position of the atom to the origin. With respect to the H_2O_2 case,[15] masses are such that difference between valence and orthogonal coordinates is much smaller.

Consider Fig. 5. The potential describing the system depends on the four coordinates (*r*, α, β, and γ), and has the following symmetry properties:

$$V(r;\alpha,\beta,\gamma) = V(r;\alpha,\pi-\beta,-\gamma) = V(r;-\alpha,\pi-\beta,\gamma)$$
$$= V(r;-\alpha,\beta,-\gamma),$$

and can be represented as a sum of two terms: An external contribution $V_{ext}(r;\alpha,\beta)$ depending on the position of the rare gas atom with respect the center of mass of the molecule, and an intermolecular contribution $V_{int}(r;\gamma)$ depending on distance *r* and the dihedral angle γ,

$$V = V_{ext}(r;\alpha,\beta) + V_{int}(r;\gamma).$$

In Ref. 18, we also discussed the use of combinations of complex-valued Wigner *D*-functions[33,34] to obtain a complete orthonormal set of real-valued hyperspherical harmonics $R_{MM'}^{\mu}(\alpha,\beta,\gamma)$.[35] It was shown that the potential energy can be expanded in terms of such functions as follows:

TABLE III. *Cis* and *Trans* geometric parameters for H_2S_2 with different basis sets and theory levels.

| Method	Basis set	R_{H-S} (Å)		R_{S-S} (Å)		$<_{HSS}$ (deg)		μ (D)
				Cis-Trans				
B3LYP	cc-pVDZ	1.357	1.358	2.170	2.157	96.5	92.7	1.86
	cc-pVTZ	1.343	1.345	2.147	2.136	96.5	92.9	1.65
	cc-pVQZ	1.341	1.343	2.141	2.128	96.6	93.0	1.58
	aug-cc-pVDZ	1.365	1.357	2.168	2.155	96.4	93.0	1.59
	aug-cc-pVTZ	1.344	1.345	2.147	2.135	96.5	93.0	1.54
	aug-cc-pVQZ	1.342	1.343	2.140	2.128	96.6	93.0	1.52
B3PW91	cc-pVDZ	1.355	1.356	2.147	2.136	96.6	92.7	1.98
	cc-pVTZ	1.343	1.345	2.126	2.114	96.5	92.9	1.71
	cc-pVQZ	1.341	1.342	2.120	2.108	96.6	93.0	1.63
	aug-cc-pVDZ	1.354	1.365	2.146	2.134	96.5	92.9	1.65
	aug-cc-pVTZ	1.343	1.345	2.126	2.114	96.5	93.0	1.59
	aug-cc-pVQZ	1.341	1.343	2.120	2.108	96.6	93.0	1.58
MP2(FU)	cc-pVDZ	1.346	1.346	2.144	2.135	96.3	92.5	2.03
	cc-pVTZ	1.332	1.337	2.112	2.102	96.0	92.4	1.79
	cc-pVQZ	1.332	1.333	2.103	2.092	96.2	92.5	1.74
	aug-cc-pVDZ	1.349	1.349	2.154	2.144	96.2	92.6	1.78
	aug-cc-pVTZ	1.332	1.336	2.111	2.102	96.1	92.4	1.72
	aug-cc-pVQZ	1.332	1.333	2.103	2.092	96.2	92.6	1.70
CCSD(T)	cc-pVDZ	1.353	1.354	2.168	2.157	96.0	92.5	2.02
	cc-pVTZ	1.340	1.344	2.139	2.082	95.9	92.6	1.79
	cc-pVQZ	1.339	1.341	2.124	2.112	96.1	92.8	1.73
	aug-cc-pVDZ	1.356	1.356	2.176	2.165	96.0	92.5	1.78
	aug-cc-pVTZ	1.342	1.343	2.139	2.127	96.0	92.7	1.71
	aug-cc-pVQZ	1.339	1.341	2.123	2.112	96.1	92.8	1.70
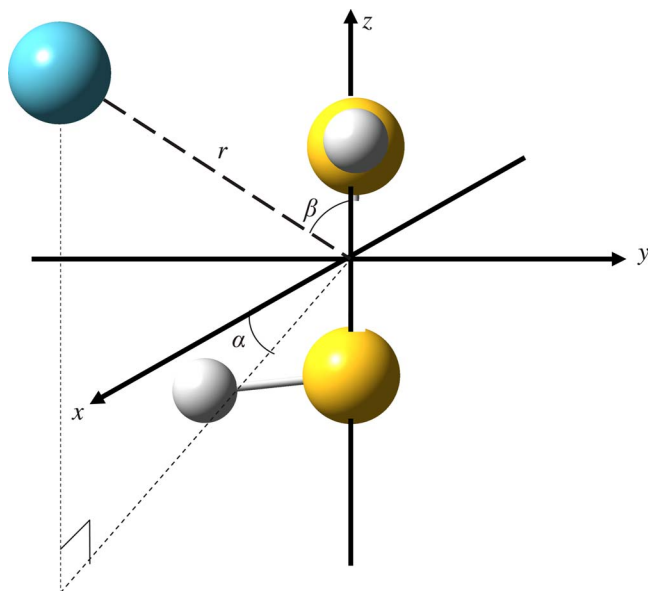
FIG. 5. (Color online) Definition of the spherical coordinates of the vector $\vec{r}=r$, β, α specifying the position of the rare gas atom for equilibrium geometry. r is the distance between the center of mass of the molecule and the rare gas atom, β is the angle between $\vec{r}$ and the z axis and α is the angle between x axis and the projection of $\vec{r}$ onto the xy plane.

$$V(r;\alpha,\beta,\gamma) = \sum V_{MM'}^{\mu}(r)R_{MM'}^{\mu}(\alpha,\beta,\gamma),$$

where $\mu = 0,1,2,\dots, M(M') = -\mu, -\mu+1, \dots, 0, 1, \dots, \mu$ and $v_{MM'}^{\mu}(r)$ are the expansion moments depending on the r coordinate. For a given geometry, at which the value of the potential is known over a range of the distance r (potential profile), the above formula reduces to a system of linear equations, to be solved for the unknown expansion moments $v_{MM'}^{\mu}(r)$.

The number of the so defined leading configurations is chosen to be 12 in this case, as in Ref. 18. For them we calculate the potential energy as a function of r enables us to determine twelve expansion moments, solving a system of 12 linear equations.

To serve as leading configurations, we have chosen, as in the case of the H$_2$O$_2$-rare gas system,[18] the molecular geometries corresponding to the *cis*, *trans*, and equilibrium geometries that for H$_2$S$_2$ corresponds to $\gamma=91.05°$. For each of these three molecular geometries, four different approach orientations of the rare-gas atom toward the H$_2$S$_2$ molecule have been considered, corresponding to $\beta=90°$ and to $\alpha = 0°$, 90°, and 180° respectively, and to $\beta=0°$ and to α undetermined.

As it has been made for H$_2$O$_2$-rare gas systems,[18] the representation of the potential energy is obtained by expansion in real hyperspherical harmonics $R_{MM'}^{\mu}(\alpha, \beta, \gamma)$ of two terms: The intramolecular contribution $V_{\text{int}}(r,\gamma)$ and the intermolecular contribution $V_{\text{ext}}(r,\alpha,\beta)$. The coefficients $w_i(\gamma)$ and the expansion moments of V_{int} are calculated according to formulas in Ref. 18 for H$_2$O$_2$. [Note that in each of the last line of Eqs. (8)–(10) of Ref. 18 the terms corresponding to the perpendicular configurations $C_\perp$, $E_\perp$, and $T_\perp$ have a wrong sign, which should be minus (−) in all three

cases.] Adaptation is needed according to the different dependence on γ for H$_2$S$_2$. Also different are the energy barriers of the *cis* and *trans* geometries used to calculate these coefficients.

For the H$_2$S$_2$ case, we have in place of Eq. (11) of Ref. 18

$$w_C(\gamma) = 0.254 + 0.5\cos\gamma + 0.246\cos(2\gamma),$$

$$w_T(\gamma) = 0.245 - 0.5\cos\gamma + 0.255\cos(2\gamma),$$

$$w_E(\gamma) = 0.5 - 0.5\cos(2\gamma).$$

For the intramolecular potential $V_{\text{int}}(r,\gamma)$, in the specific case of H$_2$S$_2$, we have [compare with Eq. (13) in Ref. 18],

$$v_{00}^{0}(r) = 0.254 v_{00}^{0}(C;r) + 0.5 v_{00}^{0}(E;r) + 0.246 v_{00}^{0}(T;r),$$

$$v_{01}^{1}(r) = 0.5 v_{00}^{0}(C;r) - 0.5 v_{00}^{0}(T;r),$$

$$v_{02}^{2}(r) = 0.246 v_{00}^{0}(C;r) - 0.5 v_{00}^{0}(E;r) + 0.254 v_{00}^{0}(T;r).$$

III. RESULTS AND DISCUSSION

A. The H$_2$S$_2$ molecule

We are interested, in general, in the conformational properties of molecules containing sulfur-sulfur bonds and began this work with theoretical study of isolated H$_2$S$_2$. The equilibrium geometric structure of hydrogen persulfide has been determined at B3LYP, B3PW91, MP2(Full) and CCSD(T) levels using different basis sets. In Table I, we present results for simplicity only for Dunning basis sets.

The H$_2$S$_2$ (or any other *R*SS*R'* compounds) is characterized by a *gauche* conformation around the S–S bond, which means that the dihedral HSSH angle is approximately 90° (Table I). The formed bond properties are mainly accounted by the *p*-character of the nonbonding electrons, which occupy mutually perpendicular *p* orbitals over each sulfur atom. The extension of these orbitals leads to superposition in the molecular orbitals. A lone pair-lone pair repulsion, inherently caused by the formation of π and π^* molecular orbitals, results in the destabilization and consequently in stretching of the S–S bond, which is maximal on *cis* and *trans* geometries (when $\gamma=0°$ and 180°, respectively), and so the destabilization is minimal when $\gamma=90°$ and 270° because of the orthogonality of the two 3*p* orbitals (Fig. 1).

For all theoretical levels and basis sets, the HSS bond angle is ∼98° (Table I). These values are in good agreement with the experimental ones reported in Refs. 36–38, and in contrast with that of Winnewisser *et al.* that underestimated the HSS angles at around 91°.[39] Generally these data are assessed on the basis that the microwave derived geometries rely on the uncertainty of the value of the HSS angle, which serves as reference. In fact, the localization of hydrogen atoms in the presence of heavy atoms is often problematic by diffraction techniques. Since the bond lengths derived from rotational constants are interrelated with the bond angles, an erroneous determination of the latter will affect other param-

eters. The torsional angles are weakly correlated with other geometrical parameters and appear internally consistent. Regarding this discussion see Refs. 40 and 41.

Theory levels and basis sets utilized in Table I accomplish a good representation of the equilibrium geometry of the system. Preliminary studies have shown us that the inclusion of polarization functions is crucial for the accurate determination of geometrical parameters. For example, the use of Pople basis sets of the type 6-311++G overestimates the SS bond length by 0.2 Å, and the dihedral angle by $\sim 3°$, with accompanying variation of dipole moment. Larger basis sets such as 6-311++G $(2df, 2pd)$ yield comparable results both with the experimental values and with those by Dunning-type basis sets.

Regarding specific features of molecular orbitals for H_2S_2 in the equilibrium geometry, a maximal stabilization arises because of the overlap which occurs between each pair of free electrons with the adjacent molecular orbital of σ^* type of HS. Two electronically degenerate conformations are possible and they are antipodal with respect to the S–S bond (Fig. 1). The rotational barriers around the SS bonds depend on the dihedral angle according to similar consideration regarding the molecular orbitals. Although there are variations in the measured and calculated barriers with different methodologies (see Table II and Ref. 40), the *cis* barriers are consistently larger than the *trans* ones.

The geometrical parameters of the transitional *cis* and *trans* structures, which are shown in Table III, indicate a distortion of the equilibrium geometry. For MP2(FU)/aug-cc-pVTZ results, the calculated values of the S–S bond lengths appear larger by 0.043–0.052 Å when compared with the equilibrium length (2.059 Å), and angles HSS appear smaller by 1.6° and 5.3°, for *trans* and *cis* geometries.

For all methods, the HS bond length appears not to vary appreciably with the geometry, ranging from 1.33 to 1.37 Å, around an average of 1.35 Å. Regarding the SS bond length, there is a stretching, moving from the equilibrium to the *cis* and *trans* geometries by 0.05 Å on the average. The HSS angles are reduced by 2° and 6°, for *trans* and *cis* geometries, in comparison with the equilibrium structure. The effect of the basis sets is to reduce bond lengths and dipole moment when we used triple and quadruple-zetas. The inclusion of diffuse function has little effect on the geometrical parameters but is important to determine the dipole moments (Fig. 4 and Sec. III D).

B. *Cis* and *trans* barriers

The *cis* and *trans* barrier heights are shown in Table II. Regarding the employed basis sets, the use of the smallest of the series of correlation consistent basis sets developed by Dunning, the cc-PVDZ, produced unsatisfactory results for the *trans* barriers independently of the utilized level of theory. A maximum deviation ~ 230 cm^{-1} with this basis set was observed with the coupled cluster method. The expansion of the series up to triple and quadruple-zetas leads to an increase of both the *cis* and *trans* barrier heights, but is not sufficient to improve the quality of results (see Table II).

The comparison among several theory levels shows that B3LYP and CCSD(T) methods underestimate barrier heights and mutually agree, independently of the Dunning basis sets used. The B3PW91 method produced, with all basis sets, *cis* barrier height in agreement with experiment, while only the aug-cc-pVTZ basis set leads to acceptable results for *trans* barriers. The better set of results was observed for MP2, including all electrons. For all aug-cc-pVXZ basis sets, good agreement was found for both *cis* and *trans* barriers, while only the cc-pVTZ basis set reproduces satisfactorily the *trans* barriers. In this case, particularly appropriate was the use of a triple zeta function. So, the aug-cc-pVTZ basis set was chosen for the study of interactions with rare gases (Sec. III E).

It has to be noted that the barriers obtained and listed in Fig. 1 by the B3LYP/6-311++G $(3df, 3pd)$ methodology (*cis* and *trans* barriers 2764 and 2009 cm^{-1}, respectively) in this case are better than when we used Dunning basis sets (on the effects of Pople and Dunning basis sets, see Ref. 41. Note that what appears as the "best" results do not always come from what are objectively our best calculations, presumably because of some fortunate cancellation of errors.

C. Comparison of H_2O_2 and H_2S_2 molecules

Figure 4 shows a comparison of the potential energy profile of H_2O_2 and H_2S_2 as a function of the dihedral angle γ. The most important observation regards the much higher value for the *trans* barrier in the H_2S_2 case, while the height of the *cis* barriers is comparable in both cases. The systematic study of the dependence of *trans* barriers upon substitution of alkyl groups for hydrogens of H_2O_2 (Ref. 16) has shown that there is a correlation with equilibrium dihedral angle, so that the barrier decreases as this angle increases. The increase in the barriers in the *trans* geometry has to be ascribed to the higher lone pair-lone pair repulsion in the $3p$ diffuse orbitals of sulfur with respect to the oxygen case.[40] For H_2S_2, we also note a smaller dipole-dipole and atom-atom interactions, and decrease in SH bond polarity with respect to OH.

The difference between *trans* barriers for HOOH and HSSH had also been interpreted in terms of hyperconjugation.[29,42,43] The 90° dihedral angle of H_2S_2 reflects the pure character of p orbitals of sulfur, as well as the low electronegativity difference between H and S, which allows for partial S–S double bonding at the expense of some H–S bonding. This has to be contrasted with H_2O_2. Another possibility is the participation of $3d$ orbitals[42]

D. Dipole moment

Figure 3 shows the variation of dipole moments as a function of the dihedral angle for both H_2O_2 and H_2S_2 and Fig. 4 as a function of the basis sets and the theory levels for the latter. From Fig. 3, it is possible to see that the smaller is the dihedral angle the larger is the dipole moment for both systems. However, in H_2O_2 for the *cis* geometry, the dipole moment is almost double than that of H_2S_2. As explained earlier, the electronegativity difference between oxygen and sulfur justifies this behavior.
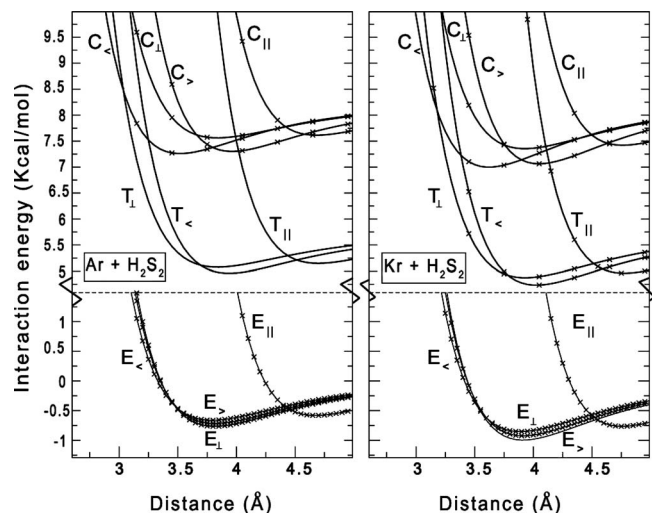
FIG. 6. He−H$_2$S$_2$ and Ne−H$_2$S$_2$ interaction energies for the leading configurations as a function of the distance of the rare gas from the center of mass of the hydrogen persulfide molecule (see Ref. 18). Crosses indicate *ab initio* points (others lie outside of the drawings) and curves are from Rydberg fits, as described in the text.

FIG. 7. Ar−H$_2$S$_2$ and Kr−H$_2$S$_2$ interaction energies for the leading configurations as a function of the distance of the rare gas from the center of mass of the hydrogen persulfide molecule (see Ref. 18). Crosses indicate *ab initio* points (others lie outside of the drawings) and curves are from Rydberg fits, as described in the text.

The dipole moment is a property that has a delicate dependence on the basis set in general decreasing with the increase of the basis (see Fig. 4 and Table I). The behavior is similar for different theory levels, leading for both MP2(FU) and CCSD(T) to an overestimate with respect to experimental information, while DFT produces better agreement. Possibly an analysis in terms of torsional wave function displacements, similar to the one discussed in the H$_2$O$_2$ case,[16] may lead to a more accurate description.

E. H$_2$S$_2$-rare gas systems

For each of the H$_2$S$_2$-Rg systems (Rg=He, Ne, Ar, and Kr), we have considered the eleven leading configurations (see Sec. II B and Ref. 18) for which the atom-molecule interaction energy has been calculated at various r (the distance between the rare-gas atom and the center of mass of the H$_2$S$_2$ molecule) by the *ab initio* methods of Sec. II B. Figures 6 and 7 show both the *ab initio* energy points and the corresponding Rydberg curve fittings for the complete rare gas series and for each of the leading configurations. The leading configurations can be distinguished into three groups, according to the geometry of the H$_2$S$_2$ molecule (*cis*, *trans*, and equilibrium) and as expected, the corresponding energy curves fall in different energy ranges: Equilibrium (lower), *trans* (intermediate), and *cis* (higher energies), according to the order common to all systems.

Another common trend that can be seen is that distances of minimum energy move to higher values and the well depths increase in going from lighter to heavier atoms. [A similar trend to be quantitatively interpreted later was also observed in previous studies of H$_2$O (Ref. 12 and 19) and H$_2$S-Rg systems[20].] It is worth noting that the "perpendicular" approach ($\beta=90°$, $\alpha=90°$), whatever the geometry of the molecule ($E_\parallel$, $C_\parallel$, and $T_\parallel$), leads to systematically more stable systems than for the corresponding "collinear" approaches ($\beta=0°$), $E_\parallel$, $C_\parallel$, and $T_\parallel$, which are also much more repulsive. Among the *cis* geometries, the one at $\beta=90°$ and
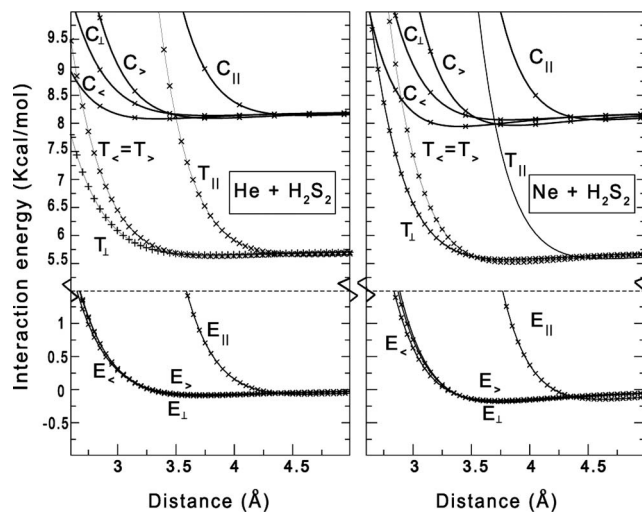
$\alpha=180°$, ($C_>$) with the atom lying on the molecule plane and approaching the molecule from the hydrogen atom side, results to be the most stable, for all the rare gas series. The difference in energy between these curves and the $C_<$ curves, with the atom at the opposite side of the hydrogens, increases from He to Kr. The $C_<$ curve exhibits the softest potential profiles. Concerning the *trans* geometries, the two directions $\alpha=0°$ and $\alpha=180°$ are equivalent by symmetry, and the $T_<$ and $T_>$ curves coincide, being the ones with the lowest energy minimum.

The equilibrium geometries are those with the lowest energy profiles. Among them, the $E_\perp$ configuration is the most stable (the lowest energy minimum) and at small distances is more repulsive than both $E_>$ and $E_<$ curves. The energy profiles corresponding to $\beta=0°$ configurations, with the atom coming along the S–S bond direction, are shifted at longer distances systematically for all the rare gas series. This can be explained by the fact that for the same value of the distance from the center of mass of the molecule, the atom can get closer to a sulfur atom when coming along the S–S bond directions, than if coming from directions perpendicular to the bond.

Figure 8 shows a comparison of the *ab initio* energy profiles for all the rare gas series, corresponding to the molecule at the equilibrium ($\gamma=91.05°$) and $\alpha=45.53°$ and $\beta=90°$, with the analogous curves as obtained from the hyperspherical expansion. This configuration was not included in the calculation of the expansion moments and the comparison is a useful test for the validity of the hyperspherical expansion. Although the difference can be appreciable in the well depths, especially for the heavier atoms, there is a substantially good agreement (very good for He and Ne), concerning the minimum energy distances and the shape of the curves. This is a remarkable fact considering that this configuration is considerably different from those included in the calculation of the hyperspherical expansion.

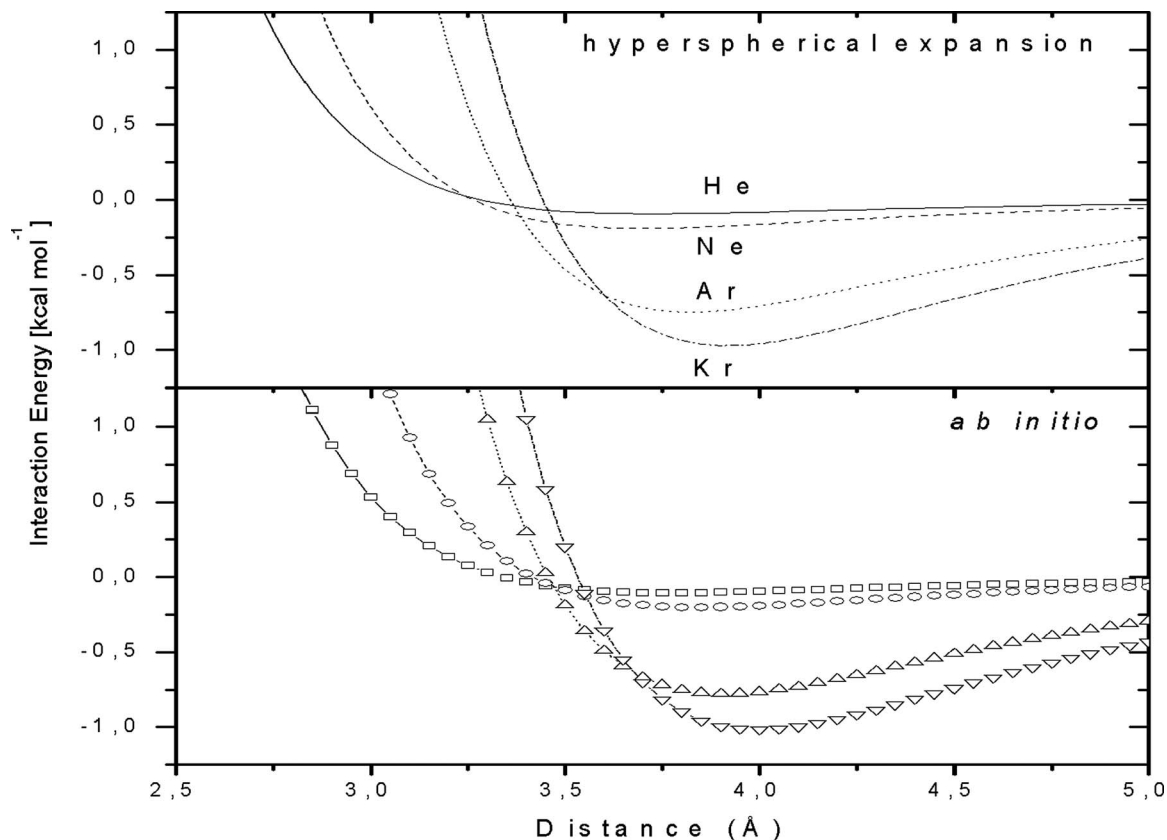Figure 9 shows the expansion moments for the H$_2$S$_2$−Ar

FIG. 8. Rare gas-H_2S_2 interaction energies as a function of the distance of the rare gas from the center of mass of the hydrogen persulfide molecule, for the equilibrium ($\gamma=91.05°$) geometry and the rare gas atom approaching from a direction given by $\beta=90°$ and $\alpha=45.53°$. Lower panel: Crosses indicate *ab initio* points (others lie outside of the drawing) and curves are from Rydberg fits, as described in the text. Upper panel: Curves indicate hyperspherical expansion representation as described in the text.

interaction, as a function of the distance from the molecule center of mass. The isotropic part of the potential, referred to the *cis*, *trans*, and equilibrium geometry of H_2S_2, is plotted along with its value averaged over the same three molecular geometries, using the w coefficients (see Ref. 18). Additionally, the contribution of the anisotropy is illustrated by the moments $\bar{v}_{01}^1$ and $\bar{v}_{02}^1$. These are nearly constant in most of

the considered distance range and do not show a minimum. As expected, the isotropic terms of the potential have minima and for $r \to \infty$ asymptotically tend to the energy of the isolated H_2S_2 molecule in the *cis*, *trans*, and equilibrium geometries.

The quantity in Fig. 9, which allows comparison with other systems, is $\bar{v}_{00}^0(r)$, representing the isotropic component of the interaction, corresponding to full averaging over both internal torsional angle γ and the external angles α and β.

Table IV shows the well depth ε and the corresponding atom-molecule distance r_m. It is interesting to compare these values with other investigated systems such as H_2O,[12,19] H_2S,[20] and H_2O_2 (Ref. 18) with the rare gases. In agreement with the known correlations between van der
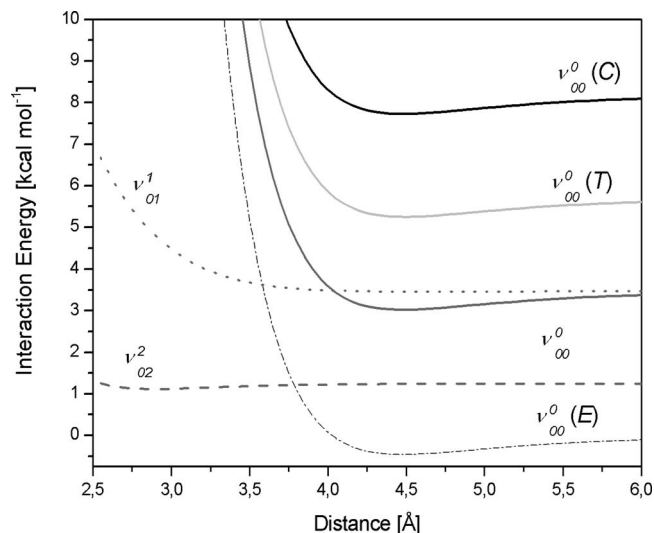

FIG. 9. Dependence on atom-molecule distance of some representative isotropic (continuous curves) and anisotropic (dashed curves) moments of the hyperspherical expansion for Ar–H_2S_2.

TABLE IV. Well depths (ε), and corresponding atom-molecule distance (r_m) of the average isotropic expansion moment $\bar{v}_{00}^{-0}$. Comparison with polarizability model, Ref. 44.

System	r_m (Å)		ε (kcal/mol)	
	Ab initio	Model[a]	*Ab initio*	Model[a]
He-H_2S_2	4.440	4.430	0.0551	0.055
Ne-H_2S_2	4.442	4.439	0.1146	0.114
Ar-H_2S_2	4.480	4.478	0.4670	0.466
Kr-H_2S_2	4.551	4.549	0.6234	0.622

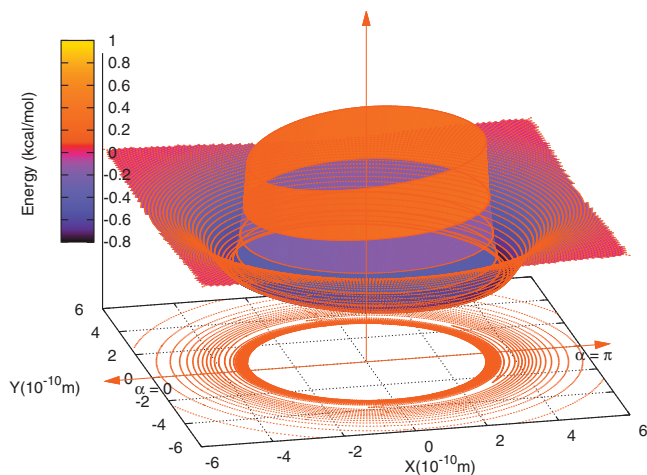[a]Polarizability for H_2S_2 44.552 (in atomic units) calculated at MP2(FU)/aug-cc-pVTZ level.

FIG. 10. (Color) Illustration of the potential energy surface for the interaction of Ar with H$_2$S$_2$, as α angle varies in the xy plane (Ref. 18) in the equilibrium geometry (γ=91.05) and the β angle is 90°. The radial coordinate in this plane of the H$_2$S$_2$ molecule. At the distance around 3.7–4.0 Å from the center of mass of the molecule, the Ar atom is in a shallow well (around −0.7 kcal/mol) slightly deeper for α=180° (atom facing the spine of the book). The other rare gas behave similarly.

Waals forces and the corresponding atomic and molecular polarizabilities[44] well depths and the corresponding distances increase with the rare gas atomic number, but the correlation (Table IV) is less quantitative than for the previously investigated systems,[45] especially regarding the distances which appear as nearly independent of the nature of the rare gas.

Regarding anisotropies, as can be seen from Figs. 6 and 7, they follow the same trends for all systems, and Fig. 9 confirms that they are generally small and slowly varying. This can be visualized in Fig. 10 where for the H$_2$S$_2$−Ar system the dependence on the torsional angle α is shown (properly freezing the angles α and β) and in Fig. 11 (where the dependence on the γ angle is shown, at fixed β=90° and α=0°). A comparison with Fig. (8) and (9) of Ref. 18, for the corresponding H$_2$O$_2$−Ar system illustrates that although small, anisotropies are larger for H$_2$S$_2$. These graphs have
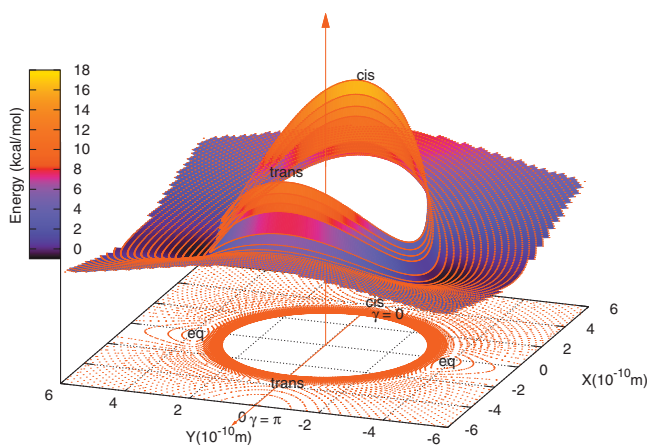

FIG. 11. (Color) View of the potential energy surface for the interaction of Ar with H$_2$S$_2$, as the torsional angle varies in the xy plane (see Ref. 18). The radial coordinate is this plane is the distance r of the Ar atom from the center-of-mass of the H$_2$S$_2$ molecule and the approach to the SS bond is α=0° and β=90°. Visible are the steep barriers of the *cis* and *trans* forms separating the two enantiomeric equilibrium geometries.

been obtained by using the full potential energy surface generated by the hyperspherical harmonics expansion, which produces a smooth interpolation among the curves corresponding to the 11 leading configurations that we have calculated in this paper. Rydberg fits to those interactions and additional information is presented as Supporting Material.[46]

IV. REMARKS AND CONCLUSIONS

The investigation reported in this paper has used modern tools of quantum chemistry to obtain information that can be of interest for the characterization of the intramolecular and intermolecular dynamics of processes involving H$_2$S$_2$. The focus has been on the torsional mode around the S–S bond. Comparisons have been made with the previously investigated torsional mode around O–O bond in H$_2$O$_2$. A following paper[47] will consider the effect of substituent groups for the H-atoms (specifically F, Cl, CH$_3$, and C$_2$H$_5$), as well as the generally higher barriers for intramolecular stereomutation transitions on the torsional levels, the associated partition functions and the rates of chirality change processes.

This paper has also considered the intermolecular interactions between H$_2$S$_2$ and the series of rare gases from He to Kr, extending previous work on H$_2$O,[12,19] H$_2$S,[20] and H$_2$O$_2$ (Ref. 18) of perspective assistance to molecular interpretation of beam scattering experiments. The derived potential energy surfaces, presented as hyperspherical harmonics expansions, can be of help for planning and analyzing collisional mechanism in chirality issues[2,14] by classical or quantum molecular dynamics.

The forthcoming paper[47] will extend this investigation to RS-R'S$'$ systems (R, R'=H, F, Cl, CH$_3$, and C$_2$H$_5$) and will report a study of intramolecular dynamics (torsional potentials, energy levels, partition functions, and chirality changing rates), along the line of analogous work[48] on H$_2$O$_2$ and its derivatives.

ACKNOWLEDGMENTS

[1] J. M. Ribó, J. Crusats, F. Sagues, J. Claret, and R. Rubires, Science **292**, 2063 (2001).
[2] A. Lombardi, F. Palazzetti, G. S. Maciel, G. Grossi, and V. Aquilanti, "The origin of chiral discrimination: Supersonic molecular beam experiments and molecular dynamics simulations of collisional mechanisms," Phys. Scr. (in press).
[3] T.-M. Su, personal communication (2006).
[4] V. Aquilanti, D. Ascenzi, D. Cappelletti, and F. Pirani, Nature (London) **371**, 399 (1994).
[5] V. Aquilanti, D. Ascenzi, D. Cappelletti, and F. Pirani, J. Phys. Chem. **99**, 13620 (1995).
[6] V. Aquilanti, D. Ascenzi, D. Cappelletti, R. Fedeli, and F. Pirani, J. Phys. Chem. A **101**, 7648 (1997).
[7] V. Aquilanti, D. Ascenzi, M. de Castro Vitores, F. Pirani, and D. Cappelletti, J. Phys. Chem. **111**, 2620 (1999).
[8] F. Pirani, D. Cappelletti, M. Bartolomei, V. Aquilanti, M. Scotoni, D. Ascenzi, and D. Bassi, Phys. Rev. Lett. **86**, 5035 (2001).
[9] F. Pirani, M. Bartolomei, V. Aquilanti, D. Cappelletti, M. Scotoni, M. Vescosi, D. Ascenzi, and D. Bassi, J. Chem. Phys. **119**, 265 (2003).
[10] V. Aquilanti, AIP Conf. Proc. **762**, 26 (2005).
[11] V. Aquilanti, M. Bartolomei, F. Pirani, D. Cappelletti, F. Vecchiocattivi, Y. Shimizu, and T. Kasai, Phys. Chem. Chem. Phys. **7**, 291 (2005).

[12] V. Aquilanti, E. Cornicchi, M. M. Teixidor, N. Saendig, F. Pirani, and D. Cappelletti, Angew. Chem., Int. Ed. Engl. **44**, 2356 (2005).

[13] D. Cappelletti, M. Bartolomei, V. Aquilanti, F. Pirani, G. Demarchi, D. Bassi, S. Iannotta, and M. Scotoni, Chem. Phys. Lett. **420**, 47 (2006).

[14] V. Aquilanti and G. S. Maciel, Origins Life Evol. Biosphere **36**, 435 (2007).

[15] G. S. Maciel, A. C. P. Bitencourt, M. Ragni, and V. Aquilanti, Chem. Phys. Lett. **432**, 383 (2006).

[16] G. S. Maciel, A. C. P. Bitencourt, M. Ragni, and V. Aquilanti, Int. J. Quantum Chem. **107**, 2697 (2007).

[17] G. S. Maciel, A. C. P. Bitencourt, M. Ragni, and V. Aquilanti, J. Phys. Chem. A **111**, 12604 (2007).

[18] P. R. P. Barreto, A. F. A. Vilela, A. Lombardi, G. S. Maciel, F. Palazzetti, and V. Aquilanti, J. Phys. Chem. A **111**, 12754 (2007).

[19] D. Cappelletti, V. Aquilanti, E. Cornicchi, M. M. Teixidor, and F. Pirani, J. Chem. Phys. **123**, 024302 (2005).

[20] D. Cappelletti, A. F. A. Vilela, P. R. P. Barreto, R. Gargano, F. Pirani, and V. Aquilanti, J. Chem. Phys. **125**, 133111 (2006); V. Aquilanti, D. Cappelletti, F. Pirani, and L. F. Roncaratti, "Velocity selection and mass spectrometric detection of an H_2S molecular beam and a collisional study of its interactions with rare gases," Int. J. Mass. Spectrom. (in press).

[21] A. Busalla, K. Blum, and D. G. Thompson, Phys. Rev. Lett. **83**, 1562 (1999).

[22] M. Musigmann, A. Busalla, K. Blum, and D. G. Thompson, J. Phys. B **32**, 4117 (1999).

[23] M. Musigmann, K. Blum, and D. G. Thompson, J. Phys. B **34**, 2679 (2001).

[24] I. Thanopulos, P. Král, and M. Shapiro, J. Chem. Phys. **119**, 5105 (2003).

[25] R. Benassi and F. Taddei, J. Phys. Chem. A **102**, 6173 (1998).

[26] M. Gottselig, D. Luckhaus, M. Quack, J. Stohner, and M. Willeke, Helv. Chim. Acta **84**, 1846 (2001).

[27] A. Bakasov, R. Berger, T.-K. Ha, and M. Quack, Int. J. Quantum Chem. **99**, 393 (2004).

[28] M. J. Frisch, G. W. Trucks, H. B. Schlegel *et al.*, GAUSSIAN 03, Revision C.02, Gaussian, Inc., Wallingford CT, 2004.

[29] C. J. Marsden and B. J. Smith, J. Chem. Phys. **92**, 347 (1988).

[30] E. Herbst and G. Winnewisser, Chem. Phys. Lett. **155**, 572 (1989).

[31] D. Yamahi, H. Kock, S. Ten-no, J. Chem. Phys, **127** 144104 (2007).

[32] S. F. Boys and F. Bernardi, Mol. Phys. **19**, 553 (1970).

[33] V. Aquilanti, S. Cavalli, C. Coletti, D. di Domenico, and G. Grossi, Int. Rev. Phys. Chem. **20**, 673 (2001).

[34] D. A. Varshalovich, A. N. Moskalev, and V. K. Kersonskii, *Quantum Theory of Angular Momentum* (World Scientific, Singapore, 1958).

[35] V. Aquilanti, S. Cavalli, and G. Grossi, J. Chem. Phys. **85**, 1362 (1986).

[36] C. J. Marsden and B. J. Smith, J. Phys. Chem. **92**, 347 (1988).

[37] M. D. Harmony, V. W. Laurie, R. L. Kuczkowski, R. H. Schwendeman, D. A. Ramsay, F. J. Lovas, W. J. Lafferty, and A. G. Maki, J. Phys. Chem. Ref. Data **8**, 619 (1979).

[38] J. Koput, Chem. Phys. Lett. **259**, 146 (1996).

[39] G. Winnewisser, M. Winnewisser, and W. Gordy, J. Chem. Phys. **49**, 3465 (1968).

[40] E. Zysman-Colman and D. N. Harp, J. Sulfur Chem. **24**, 291 (2004).

[41] K. B. Wiberg, J. Comput. Chem. **25**, 1342 (2004).

[42] D. A. Dixon, D. Zeroka, J. J. Wendeloski, and Z. R. Wasserman, J. Phys. Chem. **89**, 5334 (1985).

[43] G. N. Dolenko, E. N. Deryagina, L. P. Turchaninova, V. P. Elin, E. I. Basina, T. O. Pavlova, and V. K. Voronov, Heteroat. Chem. **6**, 623 (1995).

[44] F. Pirani, G. S. Maciel, D. Cappelletti, and V. Aquilanti, Int. Rev. Phys. Chem. **25**, 165 (2006).

[45] P. R. P. Barreto, G. S. Maciel, F. Palazzetti, and A. Lombardi, MOLEC Conference Proceedings, St. Petersburg, August 2008 (unpublished).

[46] See EPAPS Document No. E-JCPSA6-129-016839 for supporting material. For more information on EPAPS, see http://www.aip.org/pubservs/epaps.html.

[47] G. S. Maciel, M. Ragni, A. C. P. Bitencourt, V. Aquilanti, and F. V. Prudente (unpublished).

[48] G. S. Maciel, M. Ragni, A. C. P. Bitencourt, V. Aquilanti, and F. V. Prudente, "Level distributions, partition functions, and rates of chirality changing processes for the torsional mode around O-O bonds," J. Chem. Phys. (in press).